Supporting information

Defect mode passband lasing in self-assembled photonic crystal

Kuo Zhong,[†] *Liwang Liu,*[┐] *Xiaodong Xu,*[┐,‖] *Michael Hillen,*[†] *Atsushi Yamada,*[‡] *Xingping Zhou,*[£] *Niels Verellen,*[┐] *Kai Song,*[§*] *Stijn Van Cleuvenbergen,*[†] *Renaud Vallée,*[‡*] *Koen Clays*[†*]

[†]Department of Chemistry KU Leuven, Celestijnenlaan 200D, B-3001 Heverlee (Leuven), Belgium.

[┐]Department of Physics and Astronomy KU Leuven, Celestijnenlaan 200D, B-3001 Heverlee (Leuven), Belgium

[‖]Key Laboratory of Modern Acoustics, Nanjing University, Nanjing 210093, China

[‡]CNRS, University Bordeaux, CRPP, UPR 8641, 115 Avenue Schweitzer, 33600 Pessac, France

[£]School of Physics and National Laboratory of Solid State Microstructures, Nanjing University, Nanjing 210093,China.

[§]Laboratory of Bio-inspired Smart Interface Science, Technical Institute of Physics and Chemistry, Chinese Academy of Sciences, Beijing 100190, China.

Corresponding to: vallee@crpp-bordeaux.cnrs.fr; koen.clays@fys.kuleuven.be; songkai@mail.ipc.ac.cn

Experiments

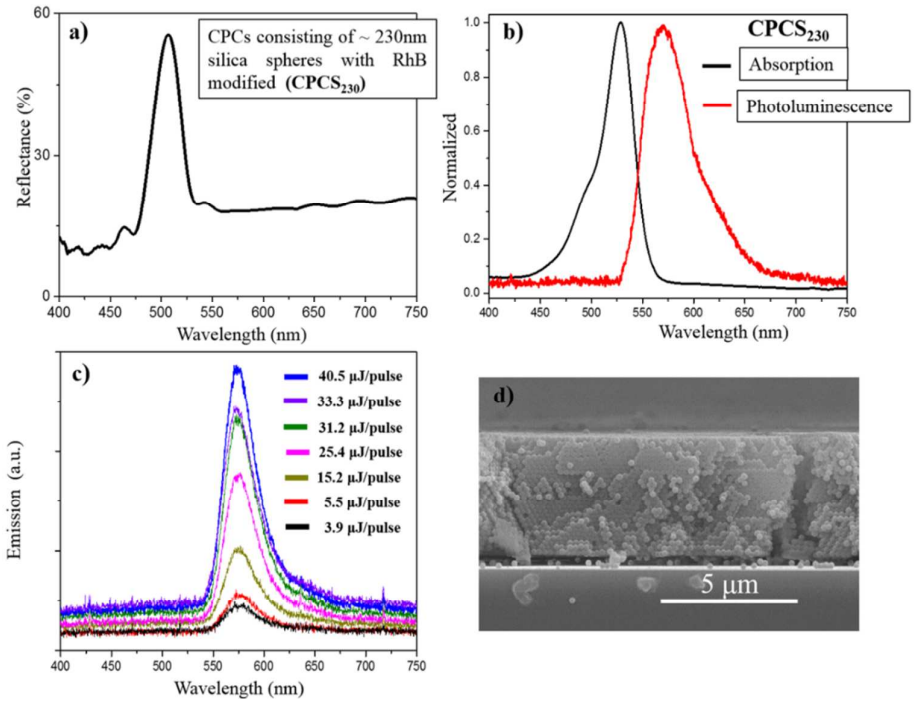

Figure S1. a) Reflectance spectrum of the CPCs consisting of RhB modified spheres with diameter of ~230 nm ($CPCs_{230}$), which acts as a reference sample since its PBG position mismatches the emission of RhB (blue-shift); b) absorption and photoluminescence of the RhB molecules in the $CPCs_{230}$. c) Corresponding fluorescence emission of the RhB emitters in such a system with various excitation energies. d) SEM image of the cross-section of the $CPCs_{230}$.

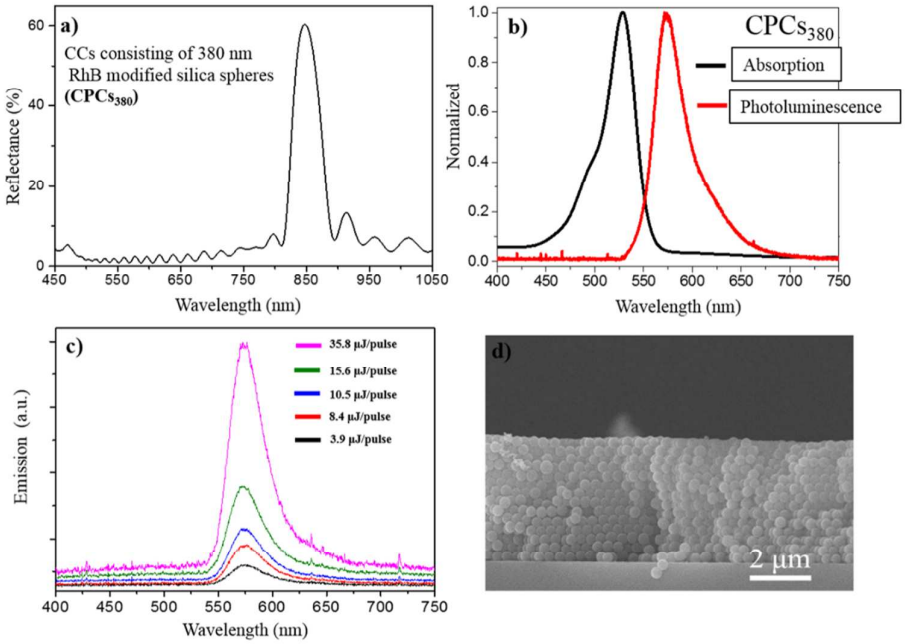

Figure S2. a) Reflectance spectra of the CPCs consisting of 380 nm RhB modified silica spheres ($CPCs_{380}$), which acts as a reference sample since its PBG position mismatches the emission of RhB (red-shift). b) absorption and photoluminesence of RhB in the $CPCs_{380}$. c) Corresponding fluorescence emission of CCs_{380} with various excitation energies. d) SEM image of the cross-section of the $CPCs_{380}$.

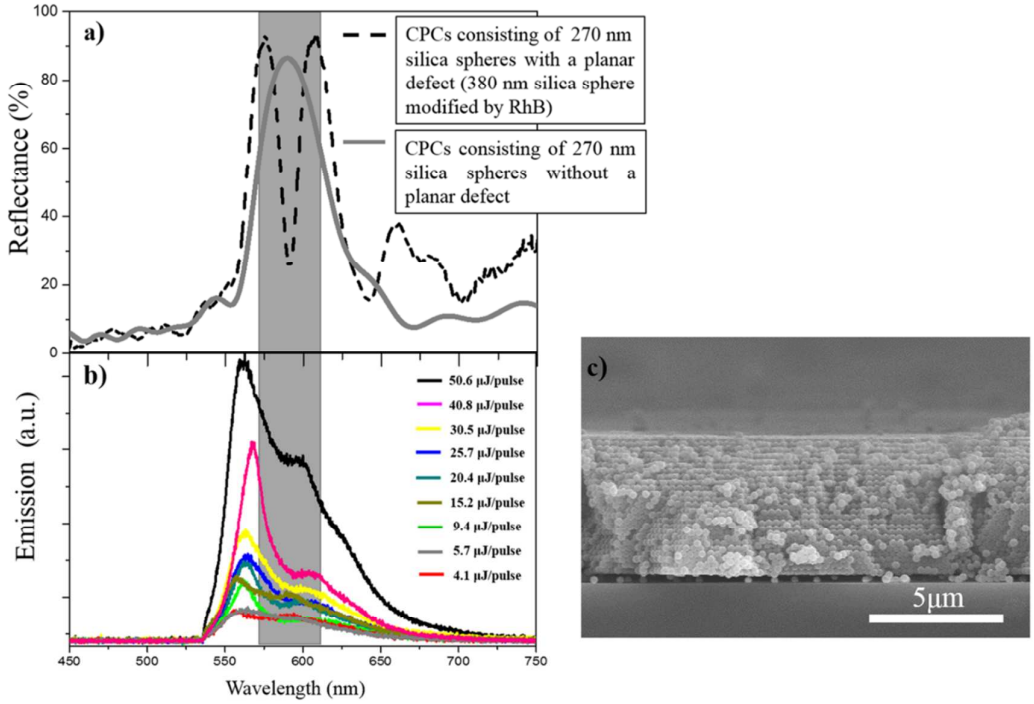

Figure S3. a) Reflectance spectra of CPCs consisting of 1) only 270 nm silica spheres

(*host* building blocks, $CPCs_{270}$, solid line) and 2) the defect layer consisting in 380 nm silica spheres inserted in between the two host structures ($CPCs_{270\text{-}380\text{-}270}$, dashed line). b) RhB fluorescence emission at various excitation energies in the $CPCs_{270}$ without defect layer. c) SEM image of the cross-section of the $CPCs_{270}$.

Simulations

Structure and gain medium:

The defect layer and the outer silica layers are structured in a unit cell of 26 x 46 x 794 grids with a grid size of 10 nm. Absorbing boundary condition are set in the (field propagating) z-direction (thickness of 750 nm at both ends) and periodic boundary conditions are implemented for the xy-directions. Nine silica layers arranged in a hexagonal closest packed lattice are put both above and below the defect layer. These host spheres have a 264 nm thickness diameter, determined on the base of the SEM results and a dielectric constant of 2.1 (refractive index: 1.45) is used. The defect layer is modeled as a slab of 298 nm thickness with an effective dielectric constant of 1.8 (refractive index: 1.34) used in order to simplify the unit cell. We confirmed the numerical accuracy and stability of our results by calculating transmission, reflection and absorption simulated spectra on a mesh with a 5 nm grid size and showed that the results are well converged by comparing them with identical ones obtained with a 10 nm grid size.

The chosen gain medium is composed of Rhodamine 6G molecules, represented as usual four-levels systems (with parameters very close but better referenced in the literature[1] than Rhodamine B, see Figure S4 and Table 1), embedded with a density of

0.1 or 0.2 [M] in the defect layer.

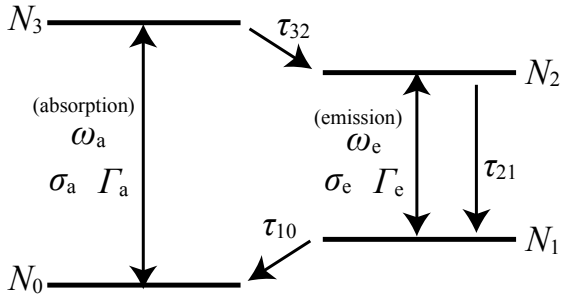

Figure S4. Four-levels system used in the dynamic analysis of the lasing process. Symbols (N, Γ, ω, τ, σ), levels (0, 1, 2 and 3) and subscripts (a and e) are defined in the text and values for the parameters are provided in Table I.

Rh6G dye molecules are structurally sufficiently close to RhB in order to nicely account for their optical and lasing properties.[1-2] The optical transition from state 0 to 3 corresponds to absorption of a photon with frequency ω_a and dephasing rate Γ_a. The one from state 2 to 1 corresponds to emission of a photon with frequency ω_e and dephasing rate Γ_e. The vibrational relaxation rates from states 3 to 2 in the electronically excited state and from states 1 to 0 in the ground state are taken into account by introducing the decay times τ_{32} and τ_{10}. The values corresponding to these parameters are collected in Table 1. The optical transitions between states 0 and 3 and between states 2 and 1 are assumed to be dipole forbidden.

Table 1. Parameters of Rhodamine 6G

Wavelength (absorption)	530 [nm]
Wavelength (emission)	580 [nm]
Relaxation time ($N_2 \rightarrow N_1$)	3.7 [ns]
Relaxation time ($N_3 \rightarrow N_2$, $N_1 \rightarrow N_0$)	100 [fs]

Resonance half-width (absorption and emission)	1/20 [fs^{-1}]
Coupling Constant (absorption)	1.51×10^{-8} [C^2kg^{-1}]
Coupling Constant (emission)	0.475×10^{-8} [C^2kg^{-1}]
Molecular density	0.1 or 0.2 [M]

The absorption and emission wavelengths and the relaxation time from N_2 (vibrational ground state in the first electronic excited state) to N_1 (vibrational excited state in the electronic ground state) are determined from experimental values.[3] The parameters of vibrational relaxation times in the electronic excited state ($N_3 \rightarrow N_2$) and ground state ($N_1 \rightarrow N_0$) are known to be small and have been taken here to be the same as the one of Rhodamine 800.[4] The coupling constants of absorption and emission are determined based on the experimental measurements of the absorption and emission cross-sections.[3]

Bloch equations for four level systems:

The Rh6G molecules, modeled as four level systems (Figure S4) obey coupled Bloch equations at each grid point in the defect layer. The time evolution of their states' population densities, $N_j(\boldsymbol{r},t)$ (j=0,.,3), is thus determined by solving equations:

$$\frac{\partial N_3}{\partial t} = \frac{1}{\hbar\omega_a}\left(\frac{\partial P_a}{\partial t} + \Gamma_a P_a\right)\cdot E_{loc} - \frac{N_3}{\tau_{32}}$$
$$\frac{\partial N_2}{\partial t} = \frac{N_3}{\tau_{32}} + \frac{1}{\hbar\omega_e}\left(\frac{\partial P_e}{\partial t} + \Gamma_e P_e\right)\cdot E_{loc} - \frac{N_2}{\tau_{21}}$$
$$\frac{\partial N_1}{\partial t} = \frac{N_2}{\tau_{21}} - \frac{1}{\hbar\omega_e}\left(\frac{\partial P_e}{\partial t} + \Gamma_e P_e\right)\cdot E_{loc} - \frac{N_1}{\tau_{10}}$$
$$\frac{\partial N_0}{\partial t} = \frac{N_1}{\tau_{10}} - \frac{1}{\hbar\omega_a}\left(\frac{\partial P_a}{\partial t} + \Gamma_a P_a\right)\cdot E_{loc}$$

The summation over the four population densities is equal to the molecular density N.

$\hbar$ is Planck constant divided by 2π. $\mathbf{E}_{loc}=[(2+\varepsilon)/3]\mathbf{E}$ represents the local electric field in the Lorentz approximation, where $\mathbf{E}$ is the incident electric field and ε is the local dielectric constant given by the host material. $\mathbf{P}_a(\boldsymbol{r},t)$ and $\mathbf{P}_e(\boldsymbol{r},t)$ denote the polarization densities of transition $0 \leftrightarrow 3$ and $1 \leftrightarrow 2$, respectively, which correspond to off-diagonal elements of the density matrix. The equations of motion of these polarization densities are:

$$\frac{\partial^2 P_i}{\partial t^2} + 2\Gamma_i \frac{\partial P_i}{\partial t} + \omega_{0,i}^2 P_i = -\sigma_i \Delta N_i E_{loc}$$

where i = a or e and $\Delta N_a(\boldsymbol{r},t)=N_3(\boldsymbol{r},t)-N_0(\boldsymbol{r},t)$, $\Delta N_e(\boldsymbol{r},t)=N_2(\boldsymbol{r},t)-N_1(\boldsymbol{r},t)$. $\boldsymbol{\sigma}_i$ is the coupling constant for process i.

This four-level system presents a simple and efficient description of laser dyes in terms of population and polarization densities responses. It takes into account the coherent effects of stimulated emission and absorption as well as the nonlinear processes of gain saturation and depletion of the transitions. The integration of nonlinear saturation and depletion make it inherently applicable beyond the regime of loss compensation where feedback and sustained pumping can lead into a state of coherent stimulated emission.

Excitation conditions

The pump and probe pulses are incident electric field plane sources, polarized along the x-axis and specified at the lower z-coordinate far outside (1000 nm) the materials, in order to avoid the occurrence of near-field effects. Their temporal profiles are sinusoids multiplied by a Gaussian. The pump pulse is varied in amplitude up to 1500

kV/cm, has a 530 nm wavelength corresponding to the absorption resonant frequency of the dye (Table 1), and a 2 ps duration (narrow bandwidth). The probe pulse is relatively weak (5 kV/cm amplitude), has a 580 nm wavelength corresponding to the emission line of the dye and a 12 fs time-width (broadband). During the pump process (5 ps in total), the dye molecules are excited, resulting in a population inversion depending on the pump power (i.e. $N_0 \rightarrow N_3$ electronic excitation and following $N_3 \rightarrow N_2$ vibrational relaxation). Then, the injected probe pulse induces stimulated emission (i.e. $N_2 \rightarrow N_1$).

Recording of the fields

The electric fields are recorded on planar detectors located on both sides of the structure (front and back side of the structure with respect to the exciting pulse). The same excitation pulse is applied to and the same fields are recorded, in an identical way, from the similar system excluding the structure (reference system), in order to determine transmission, reflection and absorption spectra. The transmission signal is obtained in the frequency domain by Fourier transforming the field detected on the back side. The reflection signal is calculated by subtraction of the front side Fourier transformed fields of the systems with and without structure. These signals are normalized by the reference signals in order to obtain the corresponding spectra. The absorption spectrum is obtained by subtracting the transmission and reflection spectra from one. The time-step in the simulation was determined owing to a Courant factor of 0.5.

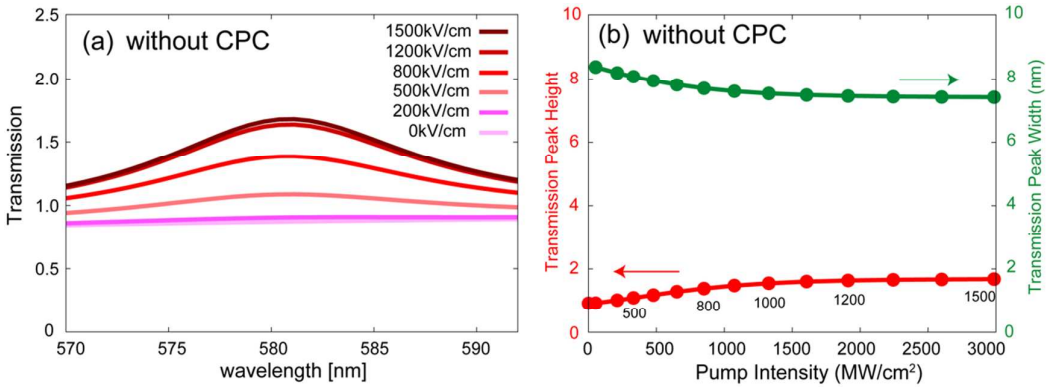

Figure S5. a) Evolution of the transmission spectra as a function of pump amplitude for a 0.2 [M] dye density system without host CPCs surrounding the defect layer and b) the in/out characteristics of this structure: the transmission peak height and width vs pump intensity. The numbers indicated on the red curve designate the field amplitude in kV/cm.

References

(1) Gaikwad, P.; Bachelard, N.; Sebbah, P.; Backov, R.; Vallee, R. A. L., Competition and Coexistence of Raman and Random Lasing in Silica-/Titania-Based Solid Foams. *Advanced Optical Materials* **2015,** *3*, 1640-1651.

(2) Bachelard, N.; Gaikwad, P.; Backov, R.; Sebbah, P.; Vallee, R. A. L., Disorder as a Playground for the Coexistence of Optical Nonlinear Effects: Competition between Random Lasing and Stimulated Raman Scattering in Complex Porous Materials. *Acs Photonics* **2014,** *1*, 1206-1211.

(3) F. J. Duarte, L. W. H., *Dye Laser Principles: With Applications*. Academic press, inc Harcourt Brace Jovanovich: **1990**.

(4) Wuestner, S.; Pusch, A.; Tsakmakidis, K. L.; Hamm, J. M.; Hess, O., Gain and Plasmon Dynamics in Active Negative-Index Metamaterials. *Philosophical Transactions of the Royal Society a-Mathematical Physical and Engineering Sciences* **2011,** *369*, 3525-3550.